Baes, M., Sobolev, S. V., Quinteros, J. (2018): Subduction initiation in mid-ocean induced by mantle suction flow. - *Geophysical Journal International*, *215*, 3, pp. 1515—1522.

DOI: http://doi.org/10.1093/gji/ggy335

Geophysical Journal International

Geophys. J. Int. (2018) **215,** 1515–1522
Advance Access publication 2018 August 13
GJI Geodynamics and tectonics

doi: 10.1093/gji/ggy335

Subduction initiation in mid-ocean induced by mantle suction flow

Marzieh Baes,[1] Stephan V. Sobolev[1,2] and Javier Quinteros[1]

[1] *Helmholtz Centre Potsdam, GFZ German Research Centre for Geosciences, Potsdam 14473, Germany. E-mail: baes@gfz-potsdam.de*
[2] *Institute of Earth and Environmental Science, University of Potsdam, Potsdam 14476, Germany*

Accepted 2018 August 11. Received 2018 July 27; in original form 2018 May 10

SUMMARY

Pre-existing weakness zones in the lithosphere such as transform faults/fracture zones and extinct mid-oceanic ridges have been suggested to facilitate subduction initiation in an intra-oceanic environment. Here, we propose that the additional forcing coming from the mantle suction flow is required to trigger the conversion of a fracture zone/transform fault into a converging plate boundary. This suction flow can be induced either from the slab remnants of former converging plate boundaries or/and from slabs of neighbouring active subduction zones. Using 2-D coupled thermo-mechanical models, we show that a sufficiently strong mantle flow is able to convert a fracture zone/transform fault into a subduction zone. However, this process is feasible only if the fracture zone/transform fault is very close to the mid-oceanic ridge. Our numerical model results indicate that time of subduction initiation depends on the velocity, domain size and location of mantle suction flow and age of the oceanic plate.

Key words: Numerical modelling;; Subduction zone processes; oceanic transform and fracture zone processes.

INTRODUCTION

Despite considerable studies on subduction initiation (McKenzie 1977; Cloetingh *et al.* 1982, 1984, 1989; Casey & Dewey 1984; Mueller & Phillips 1991; Kemp & Stevenson 1996; Toth & Gurnis 1998; Regenauer-Lieb *et al.* 2001; Hall *et al.* 2003; Gurnis *et al.* 2004; Stern 2004; Nikolaeva *et al.* 2010; Marques *et al.* 2014; Stern & Gerya 2017; Crameri *et al.* 2018) the mechanism of formation of new subduction zones is still poorly understood. Two general scenarios have been proposed for the physical mechanism of subduction initiation: spontaneous and induced (or forced; Gurnis *et al.* 2004; Stern 2004; Stern & Gerya 2017). In spontaneous view, subduction is initiated as a result of gravitational instability of the oceanic plate, which is a direct consequence of cooling of the lithosphere. Alternatively, in the forced subduction initiation, an external tectonic force such as ridge push force or forces extracting from adjacent subduction zones in the region are required to drive the oceanic plate into the mantle.

Most of previous theoretical and numerical modelling studies failed to simulate spontaneous subduction initiation using realistic model parameters (Mueller & Phillips 1991; Hall *et al.* 2003; Nikolaeva *et al.* 2010). Mueller & Phillips (1991) conducted a theoretical modelling study to investigate the possibility of subduction initiation along passive margins, transform faults/fracture zones and extinct mid-oceanic ridges. They concluded that oceanic plates cannot founder into the mantle spontaneously. They proposed that the compressional forces associated with congestion of buoyant material at a mature trench could provide a necessary extra force for subduction nucleation. They also suggested that transform faults and fracture zones represent favoured sites of trench formation. Nikolaeva *et al.* (2010), using numerical modelling, showed that spontaneous subduction initiation along passive margins is possible only if either the continental lithosphere is thinner than 75 km or continental crust is thicker than 40 km. Both of these conditions are fulfilled very rarely on the Earth, as the typical thickness of the continental crust and lithosphere along most passive margins are 35 km and more than 100 km, respectively. However, there are also some previous studies (e.g. Gerya *et al.* 2008; Dymkova & Gerya 2013), indicating that subduction can be initiated spontaneously. Gerya *et al.* (2008) carried out 2-D numerical models to investigate the cause of one-sided subduction zone on the Earth. Their model, which simulated tectonic setting of a cross-section cutting through and perpendicular to a mid-oceanic fracture zone, showed that one-sided subduction can be initiated spontaneously if the slab interface is a weak-hydrated interface with null-effective coefficient of friction and slab has a relatively high strength. Dymkova & Gerya (2013) using 2-D numerical models showed that spontaneous subduction initiation is possible as a result of porous fluid flow inside oceanic crust and along slab interface with initial high porosity and low permeability. The effective friction coefficient (yield stress/pressure) in the thrust zones in this study was almost null, that is, less than 0.01 as it is inferred from their Figs 2(a) and (b).

Alternative physical mechanism involved in subduction initiation, which is induced subduction nucleation, has been subject of several numerical studies (Toth & Gurnis 1998; Hall *et al.* 2003; Gurnis *et al.* 2004; Baes *et al.* 2011; Leng & Gurnis 2011; Lu *et al.*

2015). Toth & Gurnis (1998) explored nucleation of subduction along a dipping fault in an intra-oceanic environment. They concluded that if the shear stress along the fault is as low as a few MPa, the ridge push force alone is sufficient to form a new trench. Hall *et al.* (2003) studied possibility of formation of a new subduction zone along a fracture zone and they argued that 100 km of convergence is required to achieve a self-sustaining subduction. Gurnis *et al.* (2004) carried out similar work as Hall *et al.* (2003) and concluded that a fracture zone under compression can be converted into a self-sustaining subduction zone after approximately 100–150 km of convergence. They also claimed that an extinct mid-ocean ridge under compression can evolve into a new trench. Leng & Gurnis (2011) showed that the amount of convergence required for self-sustaining subduction initiation depends on the friction, plastic weakening and nature of boundary conditions—kinematic or dynamic boundary conditions. Baes *et al.* (2011) explored subduction initiation along newly identified weakness zones that are STEP (Subduction-Transform Edge Propagator) faults. Using numerical models they showed that STEP fault-perpendicular convergence results in a dipping shear zone along which a new subduction can evolve. They concluded that incipient subduction along a STEP fault is eased if the shear zone dips at about 45°. Lu *et al.* (2015) showed that mantle flow can cause subduction initiation on a stagnant lid. They argued that the Earth-like asymmetric subduction mode occurs for lids with friction angles of larger than 15° and moderate thermal ages. Baes & Sobolev (2017) proposed mantle suction flow as a triggering factor for subduction initiation on the present-day Earth. Using 2-D numerical models, they showed that a new subduction zone can be initiated along a passive margin or fracture zone/transform fault if a suction flow exists below or near these localities. The main focus of Baes & Sobolev (2017) was to investigate the possibility of conversion of Atlantic type of passive margins into active ones triggered by mantle flow. Extending this work, here, we aim to study factors, which help or hamper the subduction initiation process induced by mantle suction flow along transform faults/fracture zones. We explore the effect of different parameters such as age of oceanic lithosphere on both sides of transform faults/fracture zones and suction flow's velocity, domain width and location.

NUMERICAL MODEL SET-UP

We performed 281 experiments using 2-D version of SLIM3D code (Popov & Sobolev 2008) to investigate the conditions leading to formation of a subduction zone in mid-oceanic environment induced by mantle suction flow. The experiments in this study are coupled elasto-visco-plastic thermo-mechanical models in which the domains of elastic, viscous and plastic deformation are determined by the state of stress, strain rate and temperature.

Here, we established two sets of models. In the first set of experiments, the model has a 2600 km width and a 400 km depth (models M1–M255). In these models, the suction flow is simulated by imposing kinematic conditions (velocities) at the model bottom boundary (Fig. 1a). In the second series, the model domain is larger (3600 km × 1000 km; models M256–M281). In these models suction flow is induced from a sinking slab within the mantle which is initially located at the depth of 400 km (Fig. 1b). The main reason for setting up of the second series of experiments is to show that kinematic boundary conditions at the bottom boundary of the first set of experiments can simulate mantle suction flow reasonably well.

The model domain in both sets of experiments is divided into homogenous rectangular elements with the resolution of 2 km × 2 km. In the reference models of both series of experiments (models M231 and M267 in Supporting Information Table S1), an oceanic plate consisting of a 7 km crust and a 63 km lithospheric mantle is placed on the right side of the model (Figs 1a and b). On the left side of the model and below the oceanic plate lies the asthenosphere, extending to the depth of 400 km in the first and 1000 km in the second set of experiments. Mantle material on the left side of model is separated from the oceanic lithosphere by a vertical 10 km wide weakness zone, simulating a fracture zone, with a depth of 70 km, a constant viscosity of 10^{19} Pa s, which is the minimum viscosity in our models and zero friction coefficient. The choice of zero friction coefficient and low constant viscosity makes the fracture zone the weakest zone in the model. We have varied the width of fracture zone in some models (M252-M255 in Supporting Information Table S1) in order to investigate its effect on the results. In our models, an oceanic lithosphere is formed on the left side of the model as a result of plate cooling in time. We only considered the thermal effect of cooling of the plate and ignored the chemical changes in this process. These models simulate a fracture zone in mid-oceanic environment, which is located very close to the mid-oceanic ridge. In some models (M248–M255 in Supporting Information Table S1), the mantle material in the upper most portion of the left side of model is replaced by a young oceanic lithosphere. These models represent cross-sections in which fracture zones are located further away from the mid-oceanic ridge, compared to the reference models.

Table 1 lists the thermo-mechanical material properties used in our experiments. The oceanic lithospheric mantle and the asthenosphere are modelled as wet olivine (Hirth & Kohlstedt 2003). For the oceanic crust, we set a very low effective friction coefficient of 0.02. The reason is that we consider upper oceanic crust as a layer of sediments containing fluids where the high (almost lithostatic) pressure is built during deformation. Such a friction is typical for the subduction channels (Sobolev & Babeyko 2005; Osei Tutu *et al.* 2018). For the same reason we also use the material properties of a wet quartzite rheology (Ranalli 1995) for the oceanic crust. Note, however that ductile deformation in reality is not activated in the oceanic crust because of its low temperature, and therefore the entire deformation is controlled by low-friction brittle deformation mechanism. The friction coefficient of other parts of model is 0.4 (Baes & Sobolev 2017). The thermal structure of oceanic lithosphere in the reference model is based on cooling half-space model (Turcotte & Schubert 2002) for an oceanic lithosphere of 80 Myr. The temperature in the mantle is 1340 °C. In the reference model M267, a cold sinking slab is located at the depth of 400 km below the fracture zone. The temperature in the sinking slab in this model is 1000 °C. We vary the slab's temperature and slab's distance from the fracture zone in some models to explore their effects on the model outcomes (M256–M281 in Supporting Information Table S1).

The top boundary of the model is a free surface with zero stress. In the reference model of the first set of experiments, the model bottom is a free-slip boundary, except the 600 km in the middle, where we impose an average sinking velocity of 2 cm yr^{-1} (with maximum of 4 cm yr^{-1} in the centre decreasing to zero linearly towards the side boundaries, see Fig. 1a). In the second set of experiments, the bottom boundary is open except the first and last 500 km from both sides of the bottom boundary which are free-slip boundaries. In both sets of experiments the upper 50 km of the right boundary is a free-slip boundary. Below the first 50 km of the right boundary and the entire left boundary are open, allowing the net inflow and

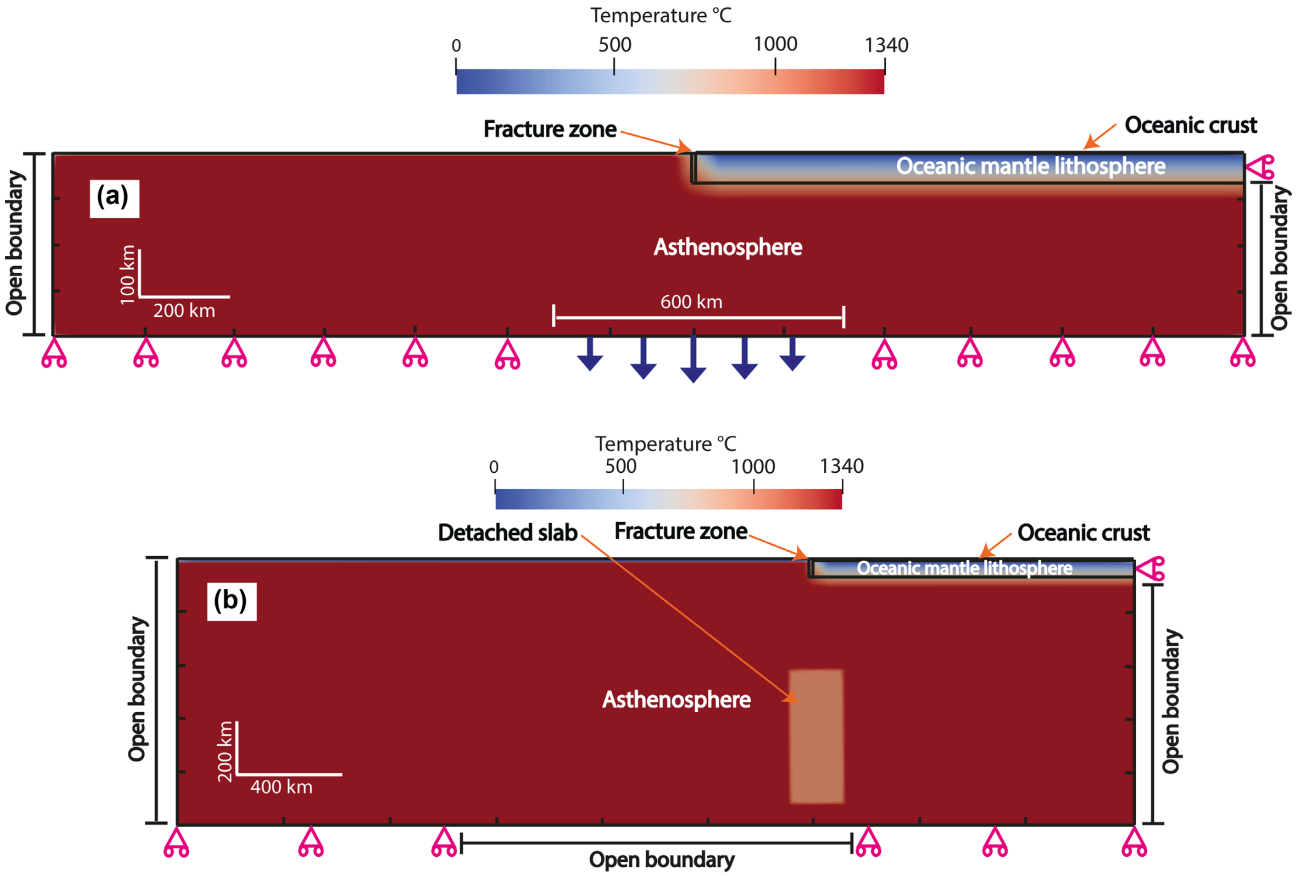

Figure 1. Initial model set-up of reference model M231 (a) and M267 (b). The colour bars indicate the temperature field.

Table 1. Material properties used in numerical experiments. ρ is density, K is bulk modulus, G is shear modulus, $\log(B_{\mathrm{Diff}})$ is pre-exponential constant for diffusion creep, E_{Diff} is activation energy for diffusion creep, V_{Diff} is activation volume for diffusion creep, $\log(B_{\mathrm{Disloc}})$ is pre-exponential constant for dislocation creep, E_{Disloc} is activation energy for dislocation creep, V_{Disloc} is activation volume for dislocation creep, n is power-law exponent for dislocation creep, μ is friction coefficient, c is cohesion, α is thermal expansivity, C_{P} is heat capacity, κ is heat conductivity and A is radiogenic heat production.

Parameter	Oceanic crust	Mantle
ρ (kg m^{-3})	2900	3300
K (GPa)	650	1290
G (GPa)	400	740
$\log(B_{\mathrm{Diff}})$ (Pa^{-1} s^{-1})	-	−8.78
E_{Diff} (kJ mol^{-1})	-	375
V_{Diff} (cm^{-3} mol^{-1})	-	2
$\log(B_{\mathrm{Disloc}})$ (Pa^{-1} s^{-1})	−15.4	−16.602
E_{Disloc} (kJ mol^{-1})	356	532
V_{Disloc} (cm^{-3} mol^{-1})	0	14
n	3.0	3.5
μ	0.02	0.4
c (MPa)	3.0	3.0
α (10^{-5} K^{-1})	2.7	3.0
C_{P} (J kg^{-1} K^{-1})	1200	1200
κ (W K^{-1} m^{-1})	2.5	3.2
A (μW m^{-3})	0.2	0

outflow to balance. Time steps of 5 kyr are used in our experiments and models evolve for 90 Myr. We vary the velocity, width and location of imposed sinking velocity, age of oceanic lithosphere and width of fracture zone to evaluate their impacts on the model results (Supporting Information Table S1).

MODEL RESULTS

Before exploring the ability of mantle flow to trigger subduction initiation we examined the possibility of spontaneous subduction initiation along a fracture zone (models M1 in Supporting Information Table S1—Supporting Information Fig. S1). The model is similar to the reference model of the first set of experiments except that here oceanic lithosphere is 40 Myr old and the entire bottom boundary is a free-slip boundary. Therefore, the only governing force in this model is gravitational force. Results of this model even after 90 Myr show almost no deformation except formation of a weak convection cell below the fracture zone. Increasing the age of the lithosphere (model M2 in Supporting Information Table S1) does not change the deformation pattern. This implies that spontaneous subduction initiation along a fracture zone is very unlikely.

The outcomes of the reference model of the first set of experiments (model M231) are shown in Fig. 2. Results show that mantle material starts to flow from left side of model towards the oceanic plate, resulting in a compressional regime near the fracture zone (Figs 2a and d). Due to this compression the young and hence weak oceanic lithosphere, which forms as a result of cooling of the mantle material on the left side of model, overthrusts the older one. In response to compression and load from the overthrusting of young oceanic lithosphere, the old oceanic lithosphere on the right side of model starts to sink into the asthenosphere (Figs 2b and e). Our criterion for subduction initiation is the time when the oceanic crust

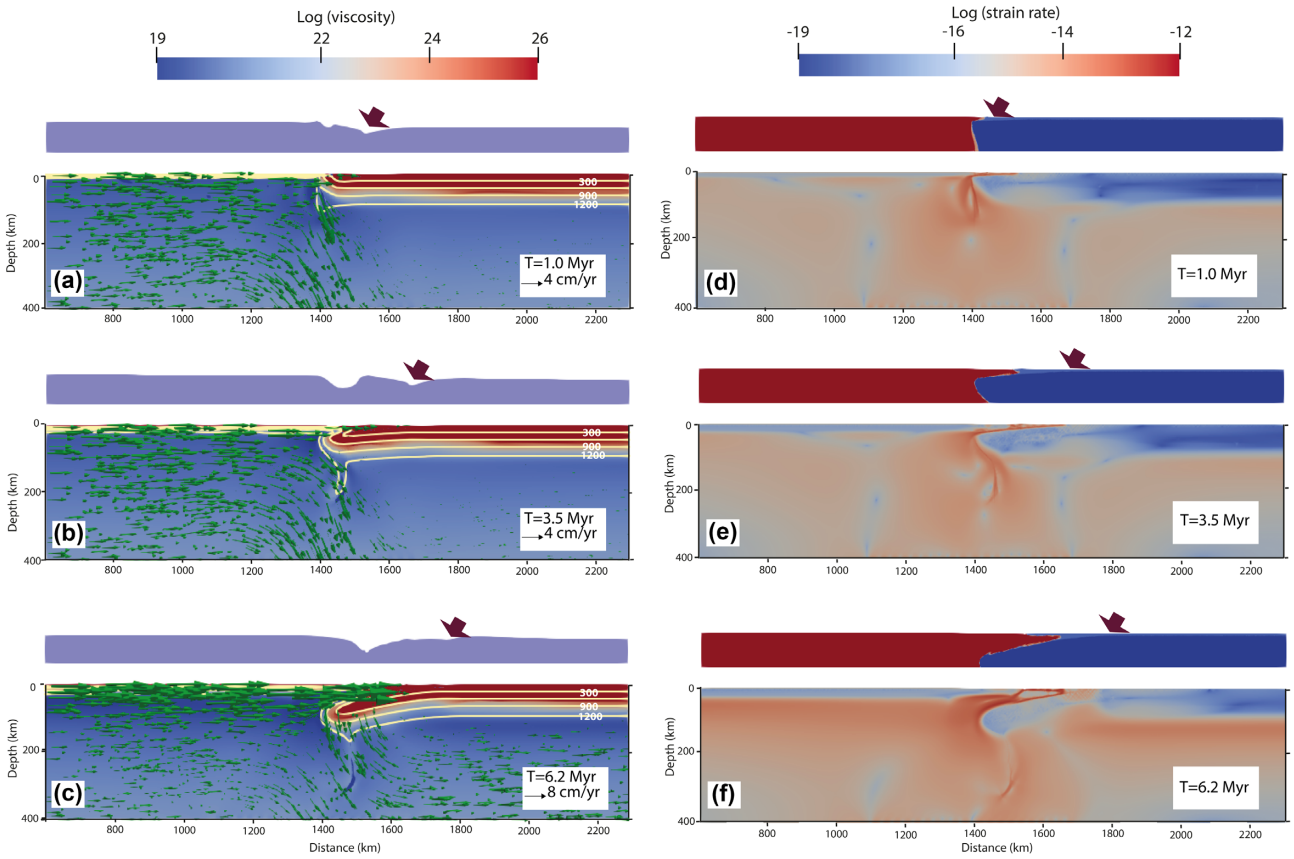

Figure 2. Results of reference model M231. In (a)–(c), upper and lower panels illustrate exaggerated surface topography and viscosity field along with velocity vectors and temperature isolines, respectively. Thick red arrows indicate location of trench. The panels in (d)–(f) show material phase field of the upper 90 km of model (upper panel) and logarithm of strain rate field (lower panel). In the upper panel of (d)–(f), the red, light-blue and dark-blue coloured regions correspond to asthenosphere, oceanic crust and lithospheric mantle, respectively.

reaches the depth of 85 km. At this moment more than 130 km of oceanic plate has been subducted into the mantle which is sufficient to form a stable subduction zone (Hall *et al.* 2003). In the reference model M231 subduction is initiated at $t = 6.2$ Myr (Figs 2c and f). During subduction of old oceanic lithosphere, parts of oceanic crust resist foundering into the mantle and overthrust on the overriding plate (upper panels in Figs 2d–f). The surface topography (upper panels in Figs 2a–c) shows that a depression develops as the old oceanic lithosphere starts to founder into the mantle and moves towards the right in time to allow the slab to hinge and sink into the greater depth. The rightward motion of this depression on the surface topography, which indicates the location of the future trench, implies that the early stage of subduction initiation is accompanied by trench retreating. During the formation of the new subduction zone the forearc area is subject to subsidence. This is due to the predicted extensional regime on the overriding plate as the oceanic plate sinks into the mantle and slab retreats. The localized depression which is formed in the forearc is vertically aligned with the tip of the slab (upper panels of Figs 2a and b) and tip of oceanic crust which is thrust on the overriding plate (upper panel of Fig. 2c) in the early and late stages of subduction initiation, respectively.

Fig. 3 shows the results of reference model M267. In this model, mantle flow induced from the sinking slab results in subduction initiation after 3.0 Myr. Comparing the results of this model with those of reference model M231, we find that the pattern of deformation in both models is very similar. This indicates that kinematic boundary conditions can simulate suction flow reasonably well.

Models simulating a fracture zone far away from the ridge (M248–M255 in Supporting Information Table S1) do not result in subduction initiation. In these models, similar to the models for exploring spontaneous subduction initiation, there is not much deformation at the lithospheric level, even after 90 Myr. Older oceanic lithosphere (M250–M251) and wider weakness zone (M252–M255) do not change the deformation pattern. This indicates that mantle suction flow is not able to trigger subduction initiation along fracture zones which are located far from the ridges.

DISCUSSION

Using numerical models, we have shown that mantle flow can be an effective triggering factor to initiate a subduction zone along a fracture zone located very close to a mid-oceanic ridge. Fig. 4 illustrates the results of models with different velocities, locations and widths of mantle flow for oceanic lithospheres of 20, 30, 40 and 80 Myr. It shows that if mantle suction flow acts on a narrow region, the subduction is initiated only if the vertical suction velocity is high. Location of such a narrow suction flow to trigger subduction initiation depends on the age of oceanic lithosphere. For young oceanic lithospheres (e.g. 20 Myr—Fig. 4a) subduction can be induced by a narrow mantle suction flow if it is located below the future overriding plate or fracture zone. In contrast, suction flow triggers subduction of old oceanic lithosphere (80 Myr—Fig. 4d) more efficiently if it is located below the future subducting plate. This is due to the bending resistance of the lithosphere which increases

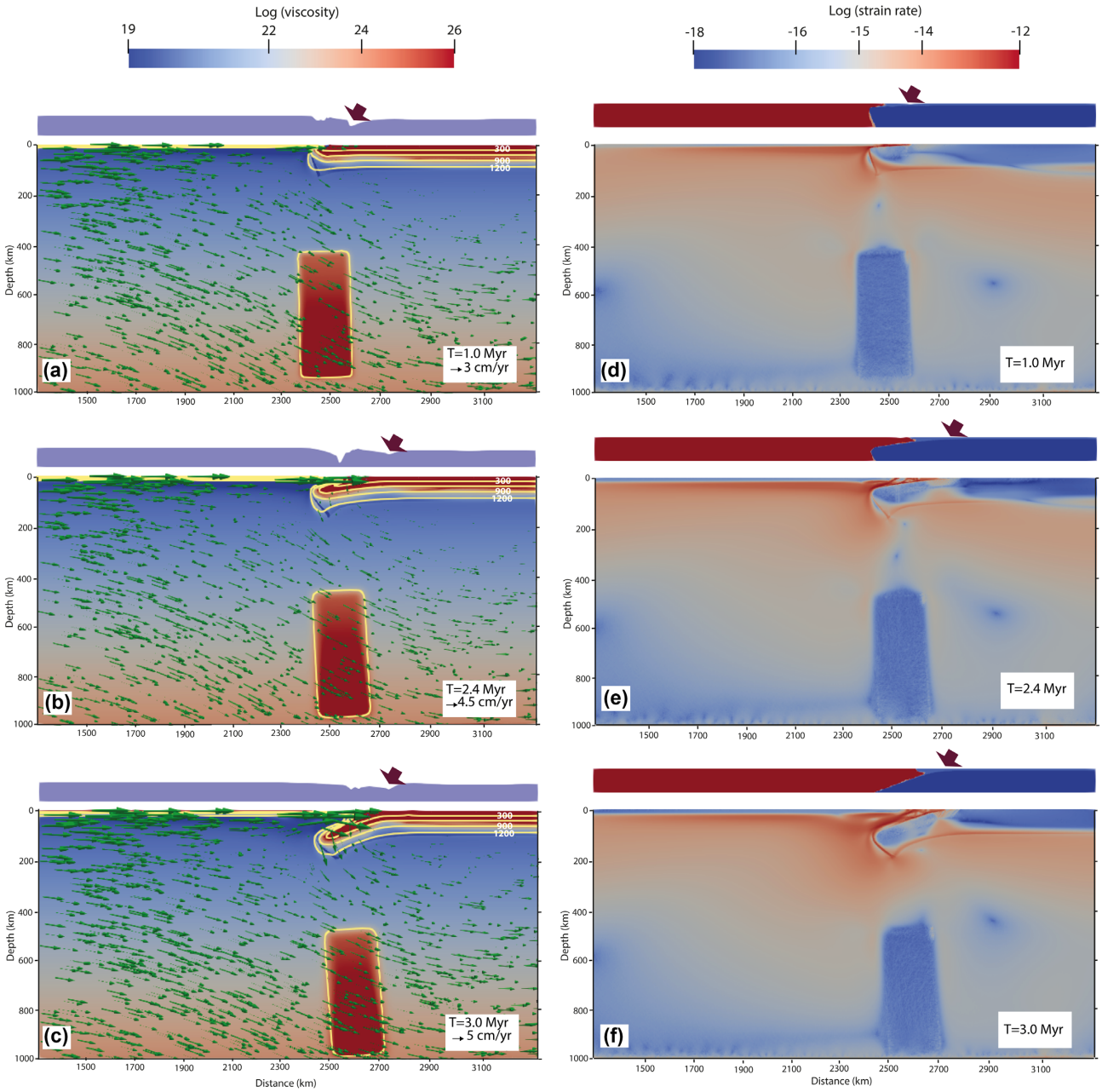

Figure 3. Results of reference model M267. The description of panels is similar to Fig. 2.

with its ageing. This resistive force can be overcome effectively if suction flow exists below the future subducting plate.

Model results of our experiments with no mantle suction flow (models M1 and M2 in Supporting Information Table S1) show that spontaneous subduction initiation is unlikely and some external forces are needed to trigger the formation of a new subduction zone. This is in good agreement with the previous studies (e.g. Mueller & Phillips 1991; Hall *et al.* 2003), but it is seemingly in contradict with modelling results of Gerya *et al.* (2008). We infer that the reason for success of Gerya *et al.* (2008) in modelling of spontaneous subduction initiation was the assumption of zero friction coefficient for the hydrated slab interface. In our models, the slab interface is lubricated by the oceanic crust with the low (0.02) but non-zero friction coefficient, which is more realistic. So, based on previous modelling results and results of this study, it is clear that spontaneous subduction initiation at oceanic fracture zones/transform faults is controversial, even in 2-D settings. We note, however, that all new subduction zones are located close to the location of the older subduction zones (Collins 2003), indicating the highly possibility of subduction initiation induced by mantle suction flow, while spontaneous initiation setting is likely rather unrealistic.

In all successful models, subduction initiation is preceded by overthrusting of younger oceanic lithosphere and extension near the future plate boundary. This is in accordance with previous studies (Kemp & Stevenson 1996; Stern 2004; Nikolaeva *et al.* 2010), indicating that subduction initiation is accompanied by a tensile regime near the plate interface. A direct consequence of this extensional regime is the subsidence of the forearc area, which can be inferred from surface topography (Buiter *et al.* 2001; De Franco *et al.* 2007).

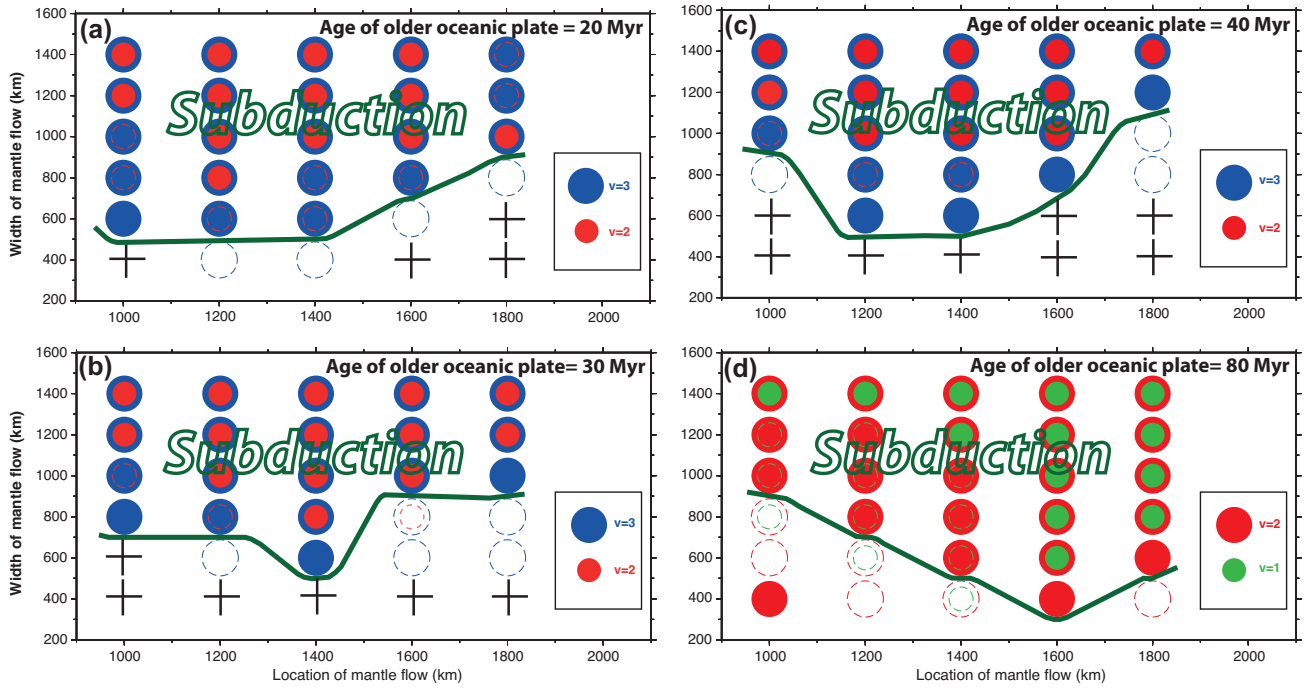

Figure 4. Sensitivity of model results to velocity, location and width of mantle suction flow for oceanic lithospheres of 20 (a), 30 (b), 40 (c) and 80 (d) Myr. Blue, red and green circles stand for average velocity of 3, 2 and 1 cm yr^{-1}, respectively. The dashed circles refer to the models with unstable results (see Supporting Information Table S1), while '+' means no subduction initiation. The fracture zone in all models is located at 1400 km.

During the early stage of the formation of a new subduction zone parts of oceanic crust do not descend into the mantle and are thrust over the overriding plate (Figs 2 and 3). This can be interpreted as the origin of ophiolites in the forearc area. It is in accordance with Stern (2004) and Dymkova & Gerya (2013) indicating that subduction initiation along a transform fault/fracture zone in the mid-ocean can originate ophiolites. Stern (2004) and Dymkova & Gerya (2013) proposed that subduction nucleation results in seafloor spreading in the forearc, which creates ophiolites. In this study, we suggest that congestion of oceanic crust at the trench and eventually thrusting of unsubducted oceanic crust on the overriding plate during the early stage of subduction initiation may be also responsible for the formation of ophiolites in forearc area.

Time of subduction initiation depends on several parameters such as age of oceanic lithosphere and width, location and velocity of mantle suction flow. Fig. 5 shows the relationship between location and width of mantle flow and time of subduction initiation for oceanic lithospheres of 20, 30, 40 and 80 Myr. This figure shows that an older oceanic lithosphere accelerates subduction nucleation process. This is in accordance with previous studies (e.g. Mckenzie 1977; Mueller & Phillips 1991; Hall *et al.* 2003; Gurnis *et al.* 2004) indicating that negative buoyancy of an oceanic plate, which increases with ageing, facilitates subduction initiation. Compared to younger lithospheres, lower velocity and narrower mantle flows are able to trigger subduction initiation of old oceanic lithospheres. Fig. 5 also shows that subduction nucleation is speeded up by a wider mantle flow. It becomes even faster when a wide mantle suction flow is centred exactly below the fracture zone (orange curves in Fig. 5). Time of subduction initiation increases by increasing of distance between suction flow and mid-oceanic fracture zone. Note that our experiments are the 2-D cross-sections. We speculate that subduction initiation may take much longer in real 3-D situation. It may also need a higher velocity and wider mantle flow in order to bend an oceanic plate and initiate subduction.

Models simulating cross-sections far away from the mid-oceanic ridge (M248–M255 in Supporting Information Table S1) failed to form a new subduction zone. We conclude that mantle flow can act as a triggering factor in subduction initiation along a fracture zone only if it is located close to the mid-oceanic ridge. Other compressional forces resulting from interaction with other plates (Hall *et al.* 2003; Gurnis *et al.* 2004) or crustal heterogeneities at neighbouring old subduction zones (Mueller & Phillips 1991) can play an efficient role in the conversion of fracture zones into subduction zones far away from ridges.

We believe that there are at least two localities on the Earth where the mantle flow triggered subduction nucleation in an intra-oceanic environment. Below, we briefly explain the geological evolution of these converging boundaries, which are the Sandwich and the Tonga–Kermadec subduction zones.

The Sandwich trench, located at the plate boundary between the South America and Antarctic, is an intra-oceanic trench in the southernmost Atlantic Ocean. The oceanic part of the South American plate subducts under the South Sandwich arc in an east–west direction. Barker (2001) indicated that the acceleration of the westward motion of the South American plate relative to the African plate resulted in the onset of convergence between the South America and the Antarctic Peninsula in the mid-Cretaceous. This led to the closure of the Rocas Verdes Basin and the formation of the Magallanes Basin and fold-thrust belt of Tierra del Fuego. Continued convergence and availability of oceanic lithosphere in the southernmost part of the South American plate resulted in the formation of the South Sandwich subduction zone along a transform fault/spreading centre at 45 Ma. At that time, the Phoenix plate was subducting beneath the Antarctic plate in the west of the Sandwich trench. We

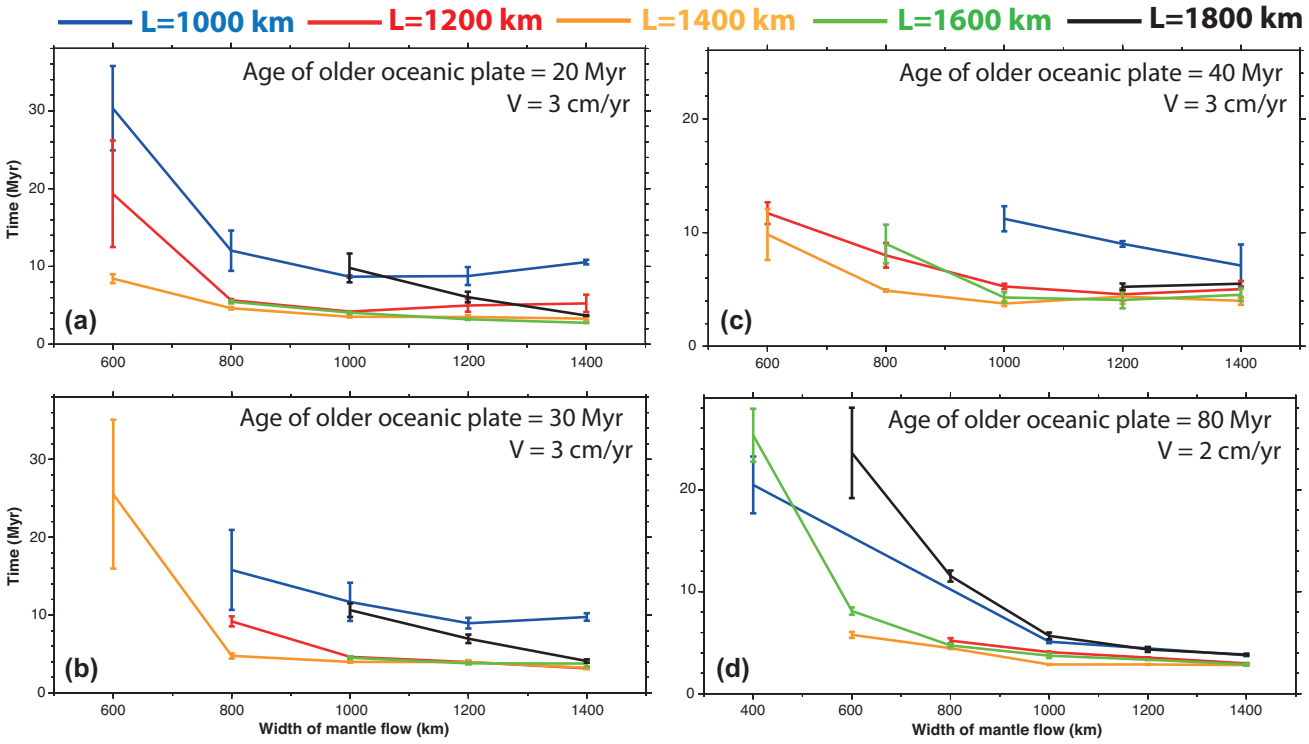

Figure 5. Time of subduction initiation versus width of the mantle flow applied for oceanic lithospheres of 20 (a), 30 (b), 40 (c) and 80 (d) Myr. Different colours of curves stand for different locations of the maximum mantle flow. $L = 1400$ corresponds to the case where mantle suction flow is exactly below the fracture zone. Error bars show the range of uncertainties.

suggest that mantle flow induced from the east-dipping subduction of the Phoenix plate, which was an active-mature subduction zone located very close to the Sandwich trench, facilitated subduction initiation. Remnants of the Phoenix subduction zone can be evidenced in the upper part of lower mantle in mantle tomographic images (e.g. Bijwaard *et al.* 1998).

The Tonga–Kermadec subduction zone, located between Australian and Pacific plates, is a self-sustaining subduction zone, which formed at approximately 45 Ma (Bloomer *et al.* 1995). It is proposed that subduction was initiated along an intra-Pacific fracture zone (Todd *et al.* 2012)/spreading centre (Eissen *et al.* 1998). Gaina *et al.* (1998) argued that Pacific motion was approximately parallel to the Norfolk ridge prior to 45 Ma while it became perpendicular afterwards. Despite loss of considerable geological record of the Pacific plate since 45 Ma, the magnetic anomalies show that the present orientation of spreading centres and magnetic lineations on the Pacific plate are perpendicular to the strike of the trench (Gurnis *et al.* 2004 and references therein), indicating the formation of subduction in an intra-oceanic weakness zone. Some of previous studies suggested that a short-lived east verging subduction zone was active in the region, very close to the location of the future Tonga trench, from 50 to 45 Ma before the formation of the oppositely dipping Tonga–Kermadec subduction zone (Kroenke 1984, Eissen *et al.* 1998). We think that the triggering factor in the formation of the Tonga–Kermadec subduction zone was the suction mantle flow coming from either the Vitiaz subduction zone, which was active in the north of the (future) Tonga–Kermadec trench or the east-dipping short-lived subduction zone. Evidence of former subduction zones in the region can be inferred from mantle tomographic images. Chen & Brudzinski (2001), using mantle tomography, showed evidence for a large-scale remnant of subducted lithosphere beneath Fiji, which they attributed to the detached slab of past subduction of the Pacific plate along the Vitiaz trench. Moreover, *P*-wave tomographic images from the southwest Pacific region show high-velocity anomalies in both upper and lower mantle (Schellart & Spakman 2012), which indicate that large amounts of old and cold slab have been subducting in the past 50–100 Myr.

CONCLUSIONS

In this study, we have shown that a transform fault/fracture zone can convert into a converging plate boundary provided that a mantle suction flow is located below it. Our numerical model results indicate that the early stage of subduction nucleation is accompanied by trench retreat and extension of the overriding plate. Resistance of portions of oceanic crust to subduction, which eventually results in thrusting of unsubducted oceanic crust on the overriding plate during the early stage of subduction initiation leads to formation of ophiolites in forearc area. Subduction initiation induced by mantle suction flow can be speeded up by the increase of extent and intensity of mantle flow. Mantle flow below oceanic lithosphere is more efficient in triggering subduction initiation if the oceanic lithosphere is old ($\geq$80 Myr). In contrast, flow below the overriding plate plays a key role when the oceanic lithosphere is young. The results show that our scenario of conversion of transform faults/fracture zones into subduction zones induced by mantle suction flow is valid only if suction flow is below a fracture zone/transform fault which is located very close to the mid-oceanic ridge.

ACKNOWLEDGEMENTS

We thank Taras Gerya and Fabio Crameri for their constructive and fruitful comments. MB designed the study, conducted the numerical

experiments and interpreted the results. SVS designed the study and interpreted the results. JQ helped to set up the numerical models and interpreted the results. All authors wrote the paper and discussed the results.

REFERENCES

Baes, M., Govers, R. & Wortel, R., 2011. Subduction initiation along the inherited weakness zone at the edge of a slab: insights from numerical models, *Geophys. J. Int.,* **184**(3), 991–1008.

Baes, M. & Sobolev, S.V., 2017. Mantle flow as a trigger for subduction initiation: a missing element of the Wilson cycle concept, *Geochem. Geophys. Geosyst.,* **18**(12), 4469–4486.

Barker, P.F., 2001. Scotia Sea regional tectonic evolution: implications for mantle flow and palaeocirculation, *Earth-Science Reviews,* **55,** 1–39.

Bijwaard, H., Spakman, W. & Engdahl, E.R., 1998. Closing the gap between regional and global travel time tomography, *J. geophys. Res.,* **103**(B12), 30 055–30 078.

Bloomer, S.H., Taloy, B., Macleod, C.J., Stern, R.J., Fryer, P., Hawkins, J.W. & Johnson, L., 1995. Early arc volcanism and the ophiolite problem: a perspective from drilling in the western Pacific, in *Active Margins and Marginal Basins of the Western Pacific,* pp. 1–30, eds Taylor, B. & Natland, J., American Geophysical Union.

Buiter, S., Govers, R. & Wortel, R., 2001. A modelling study of vertical surface displacements at convergent plate margins, *Geophys. J. Int.,* **147,** 415–427.

Casey, J. & Dewey, J., 1984. Initiation of subduction zones along transform and accreting plate boundaries, triple-junction evolution, and forearc spreading centres—implications for ophiolitic geology and obduction, *Geol. Soc. Lond. Spec. Publ.,* **13**(1), 269–290.

Chen, W-P & Brudzinski, M.R., 2001. Evidence for a large-scale remnant of subducted lithosphere beneath Fiji, *Science,* **292,** 2475–2479.

Cloetingh, S., Wortel, M. & Vlaar, N., 1984. Passive margin evolution, initiation of subduction and the Wilson cycle, *Tectonophysics,* **109**(1), 147–163.

Cloetingh, S., Wortel, R. & Vlaar, N., 1989. On the initiation of subduction zones, *Pure appl. Geophys.,* **129**(1–2), 7–25.

Cloetingh, S.A.P.L., Wortel, M. & Vlaar, N., 1982. Evolution of passive continental margins and initiation of subduction zones, *Geol. Ultraiecrina,* **29,** 1–111.

Collins, W., 2003. Slab pull, mantle convection, and Pangaean assembly and dispersal, *Earth planet. Sci. Lett.,* **205**(3), 225–237.

Crameri, F., Conrad, C.P., Montési, L. & Lithgow-Bertelloni, C.R., 2018. The dynamic life of an oceanic plate, *Tectonophysics,* in press.

De Franco, R., Govers, R. & Wortel, R., 2007. Numerical comparison of different convergent plate contacts: subduction channel and subduction fault, *Geophys. J. Int.,* **271,** 435–450.

Dymkova, D. & Gerya, T., 2013. Porous fluid flow enables oceanic subduction initiation on Earth, *Geophys. Res. Lett.,* **40,** 5671–5676.

Eissen, J-P, Crawford, A.J., Cotton, J., Meffre, S., Bellon, H. & Delaune, M., 1998. Geochemistry and tectonic significance of basalts in the Pony Terrane, New Caledonia, *Tectonophysics,* **284,** 203–219.

Gaina, c., Müller, R.D., Royer, J-Y, Stock, J., Hardebeck, J. & Symonds, P., 1998. The tectonic history of the Tasman Sea: a puzzle with 13 pieces, *J. geophys. Res.,* **103,** 12 413–12 433.

Gerya, T.V., Connolly, J.A.D. & Yuen, D.A., 2008. Why is terrestrial subduction one-sided? *Geology,* **36,** 43–46.

Gurnis, M., Hall, C. & Lavier, L., 2004. Evolving force balance during incipient subduction, *Geochem. Geophys. Geosyst.,* **5**(7).

Hall, C.E., Gurnis, M., Sdrolias, M., Lavier, L.L. & Müller, R.D., 2003. Catastrophic initiation of subduction following forced convergence across fracture zones, *Earth planet. Sci. Lett.,* **212**(1), 15–30.

Hirth, G. & Kohlstedt, D., 2003. Rheology of the upper mantle and the mantle wedge: a view from the experimentalists, in *Inside the Subduction Factory,* pp. 83–105, ed. Eiler, J., American Geophysical Union.

Kemp, D.V. & Stevenson, D.J., 1996. A tensile, flexural model for the initiation of subduction, *Geophys. J. Int.,* **125**(1), 73–93.

Kroenke, L.W., 1984. *Cenozoic Tectonic Development of the Southwest Pacific,* Technical Secretariat of CCOP/SOPAC c/o Mineral Resources Department.

Leng, W. & Gurnis, M., 2011. Dynamics of subduction initiation with different evolutionary pathways, *Geochem. Geophys. Geosyst.,* **12**(12).

Lu, G., Kaus, B.J., Zhao, L. & Zheng, T., 2015. Self-consistent subduction initiation induced by mantle flow, *Terra Nova,* **27**(2), 130–138.

Marques, F.O., Cabral, F.R., Gerya, T.V., Zhu, G. & May, D.A., 2014. Subduction initiates at straight passive margins, *Geology,* **42,** 331–334.

McKenzie, D., 1977. The initiation of trenches: a finite amplitude instability, in *Island Arcs, Deep Sea Trenches and Back-Arc Basins,* pp. 57–61, eds Talwani, M. & Pitman III, W.C., American Geophysical Union.

Mueller, S. & Phillips, R.J., 1991. On the initiation of subduction, *J. geophys. Res.,* **96,** 651–665.

Nikolaeva, K., Gerya, T. & Marques, F., 2010. Subduction initiation at passive margins: numerical modeling, *J. geophys. Res.,* **115**(B03406).

Osei Tutu, A., Sobolev, S.V., Steinberger, B., Popov, A. & Rogozhina, I., 2018. Evaluating the influence of plate boundary friction and mantle viscosity on plate velocities, *Geochem. Geophys. Geosyst.,* **19**(G3), 642–666.

Popov, A.A. & Sobolev, S.V., 2008. SLIM3D: a tool for three-dimensional thermomechanical modeling of lithospheric deformation with elasto-visco-plastic rheology, *Phys. Earth planet. Inter.,* **171**(1), 55–75.

Ranalli, G., 1995. *Rheology of the Earth,* Springer.

Regenauer-Lieb, K., Yuen, D.A. & Branlund, J., 2001. The initiation of subduction: criticality by addition of water? *Science,* **294**(5542), 578–580.

Schellart, W.P. & Spakman, W., 2012. Mantle constraints on the plate tectonic evolution of the Tonga–Kermadec–Hikurangi subduction zone and the South Fiji Basin region, *Aust. J. Earth Sci.,* **59,** 933–952.

Sobolev, S.V. & Babeyko, A.Y., 2005. What drives orogeny in the Andes?, *Geology,* **33,** 617–620.

Stern, R.J., 2004. Subduction initiation: spontaneous and induced, *Earth planet. Sci. Lett.,* **226,** 275–292.

Stern, R.J. & Gerya, T., 2017. Subduction initiation in nature and models: a review, *Tectonophysics,* in press.

Todd, E., Gill, J.B. & Pearce, J.A., 2012. A variably enriched mantle wedge and contrasting melt types during arc stages following subduction initiation in Fiji and Tonga, southwest Pacific, *Earth planet. Sci. Lett.,* **335–336,** 180–194.

Toth, J. & Gurnis, M., 1998. Dynamics of subduction initiation at preexisting fault zones, *J. geophys. Res.,* **103**(B8), 18 053–18 067.

Turcotte, D.L. & Schubert, G., 2002. *Geodynamics,* 2nd edn, Cambridge Univ. Press.

SUPPORTING INFORMATION

Supplementary data are available at *GJI* online.

Figure S1. Results of model M1, exploring spontaneous subduction initiation.

Table S1. Description of numerical experiments.

Please note: Oxford University Press is not responsible for the content or functionality of any supporting materials supplied by the authors. Any queries (other than missing material) should be directed to the corresponding author for the article.